Metal–Organic Frameworks

DOI: 10.1002/anie.200804836

Heterogeneously Hybridized Porous Coordination Polymer Crystals: Fabrication of Heterometallic Core–Shell Single Crystals with an In-Plane Rotational Epitaxial Relationship**

Shuhei Furukawa, Kenji Hirai, Keiji Nakagawa, Yohei Takashima, Ryotaro Matsuda, Takaaki Tsuruoka, Mio Kondo, Rie Haruki, Daisuke Tanaka, Hirotoshi Sakamoto, Satoru Shimomura, Osami Sakata, and Susumu Kitagawa**

The formation of interfaces between two solid phases is of great significance in the development of new materials, because mechanical and electronic properties of materials are strongly influenced by distorted interfacial structures, leading to properties that differ from those of the individual phases. Moreover, properties of porous materials, such as gas sorption and guest-molecule accommodation, should also correlate with the interfacial structure of such materials, because guest molecules (adsorbates) first encounter the surface of the porous materials. Hence, the affinity of porous materials for guest molecules can be tuned by modifying the surface structure.[1]

Porous coordination polymers (PCPs), or metal–organic frameworks (MOFs), are an interesting class of crystalline porous materials, as it is possible to design their framework topologies and pore sizes and the functionality of the pore surfaces.[2] Recent progress of the "post-synthetic approach" allows for the pore-surface functionalities (on the inner surfaces of materials) to be altered after the lattice is constructed.[3] On the other hand, functionalization of PCP outer surfaces is a great challenge, but it is a promising methodology not only for modification of the porous properties but also for the addition of a new function to the PCP without changing the characteristic features of the PCP crystal itself,[4] resulting in the fabrication of multifunctional PCPs. One way to decorate the crystal surfaces of a PCP is to hybridize the core PCP crystal with a different shell crystal by epitaxial growth at the single-crystal level, thus creating core–shell PCP heteroepitaxial crystals. Such a lattice match promises pore connections at the interface between crystals, where the modified crystal structure should influence the mobility and diffusion of adsorbates. Such fabrication of hybridized PCP single crystals in the nanometer or micrometer regime also allows for utilization of these materials in biological systems and as sensors in electronic devices.[4,5] Although a few pioneering synthetic studies on the hybridization of extended coordination structures have been reported,[6] structural determination at the interfaces is not yet known, most likely because of the lack of a methodology, despite its significance for the design of new materials. Herein, we demonstrate the first synthesis of core–shell PCP single crystals by epitaxial growth; the structural relationship between the shell and the core was determined using surface X-ray diffraction analysis.

The key to success is to choose excellent candidates for epitaxial growth, such as the $[\{M_2(\text{dicarboxylate})_2(\text{N ligand})\}_n]$ series of PCP frameworks, wherein three components, namely the metal ions, dicarboxylate layer ligands, and bidentate nitrogen pillar ligands, can be varied without changing the original tetragonal topology (Figure 1).[7] A variety of isoreticular tetragonal frameworks with similar unit cell parameters are available. The heterometallic system chosen for hybridization consists of different metal ions with the same organic ligands: $[\{Zn_2(ndc)_2(dabco)\}_n]$[7d] (**1**) as the core crystal and $[\{Cu_2(ndc)_2(dabco)\}_n]$[7h] (**2**) as the shell crystal (ndc = 1,4-naphthalene dicarboxylate, dabco = diazabicyclo[2.2.2]octane). Note that **1** can be grown as a single crystal with cubic morphology at a scale of hundreds of micrometers, but **2** gives only microcrystalline powder. Therefore, synthesis of the reverse composition is essentially impossible.

To elucidate the growth process of the core crystal **1**, face-index analysis was carried out using single-crystal X-ray diffraction. The tetragonal framework appears as a right rectangular prism crystal with (100), (−100), (010), (0−10), (001), and (00−1) faces. The four (h00) and (0k0) surfaces can be end-capped by the layer carboxylic acid groups, whereas the two remaining (00l) surfaces are terminated by the

[*] Dr. S. Furukawa, Dr. R. Matsuda, Dr. T. Tsuruoka, Prof. S. Kitagawa
ERATO Kitagawa Integrated Pores Project (Japan)
Kyoto Research Park Bldg #3, Shimogyo-ku, Kyoto 600-8815 (Japan)
Fax: (+81) 75-325-3572
E-mail: kitagawa@sbchem.kyoto-u.ac.jp
Homepage: http://kip.jst.go.jp

Dr. S. Furukawa, Dr. R. Matsuda, Dr. M. Kondo, Prof. S. Kitagawa
Institute for Integrated Cell-Material Sciences (iCeMS)
Kyoto University, Yoshida, Sakyo-ku, Kyoto 606-8501 (Japan)

K. Hirai, K. Nakagawa, Y. Takashima, Dr. D. Tanaka, H. Sakamoto, S. Shimomura, Prof. S. Kitagawa
Department of Synthetic Chemistry & Biological Chemistry
Graduate School of Engineering, Kyoto University
Katsura, Nishikyo-ku, Kyoto 615-8510 (Japan)

Dr. R. Haruki, Dr. O. Sakata
Research & Utilization Division (Japan)
Synchrotron Radiation Research Institute/SPring-8 and CREST, JST
Kouto, Sayo, Hyogo 679-5198 (Japan)
E-mail: o-sakata@spring8.or.jp

[**] The synchrotron X-ray diffraction experiments were performed at BL13XU in the SPring-8 with the approval of the JASRI (Proposal No. 2007A1825, 2007B1771, and 2008A1574).

Supporting information for this article is available on the WWW under http://dx.doi.org/10.1002/anie.200804836.

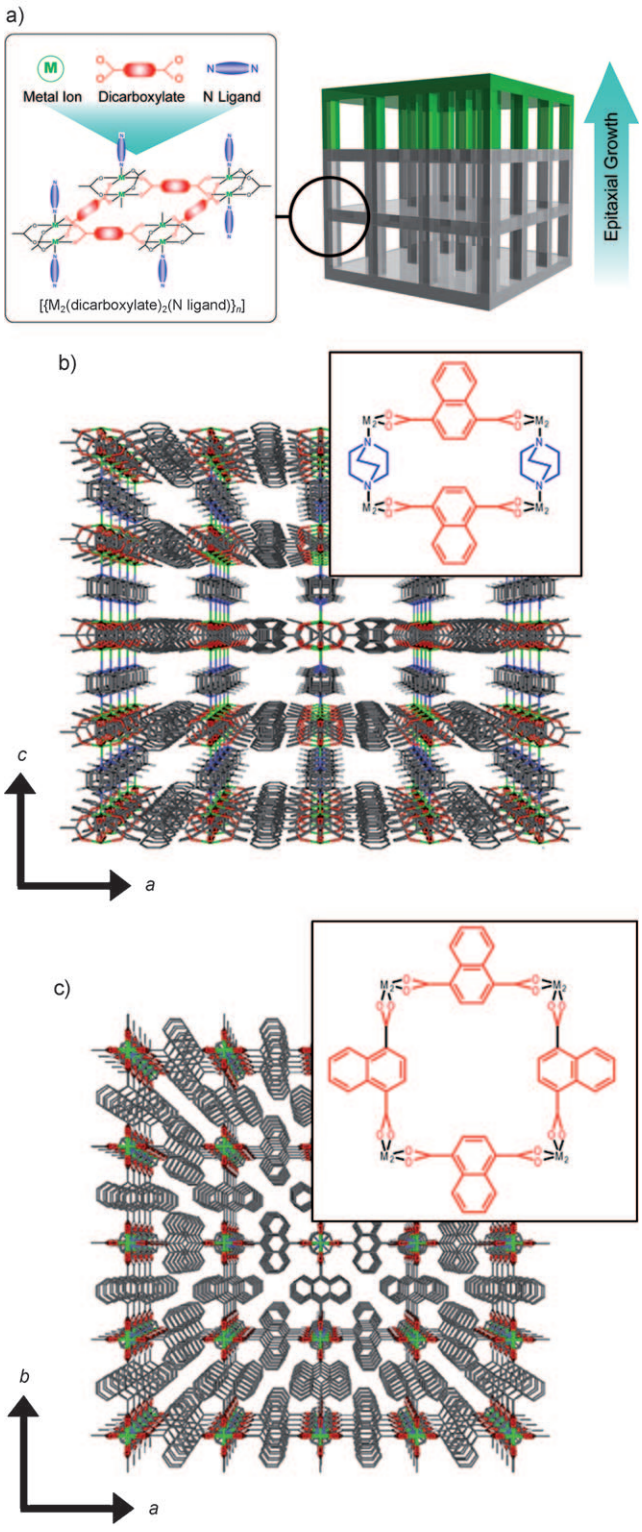

Figure 1. a) Schematic illustration of the series of frameworks $[\{M_2(\text{dicarboxylate})_2(\text{N ligand})\}_n]$. b,c) The crystal structure of **1** viewed along the *b* axis (b) and the *c* axis (c). The naphthalene moieties are disordered owing to the symmetry. The insets show the chemical structures of the (100) surface (b) and the (001) surface (c).

nitrogen pillar ligands. These ligands can be used as coordination sites to grow the shell crystal.

The hybridization of two frameworks into one single crystal has been successfully achieved by a simple solvothermal synthesis; pieces of single crystals of **1** were put into a solution of $CuSO_4{\cdot}5H_2O$, 1,4-naphthalene dicarboxilic acid, and dabco in toluene/methanol (1:1), and the solution was heated to 393 K. The core–shell crystals (**1/2**) were obtained as light greenish cubic crystals in 93% yield.[8]

Figure 2a shows an optical microscopy image of the sliced single crystal of **1/2**. The colorless core crystal is surrounded by the greenish shell crystal. Each part of the core–shell

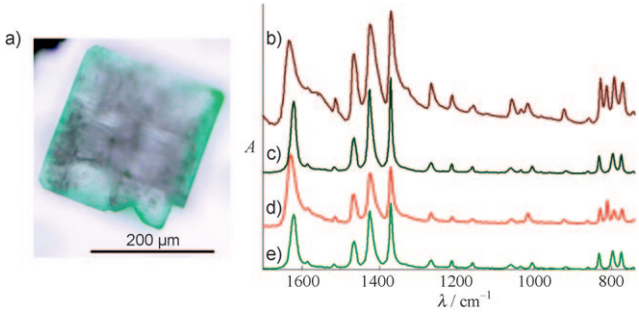

Figure 2. a) Optical microscopic image of the sliced core–shell crystal **1/2**. b–e) IR spectra by microscopic attenuated total reflection (ATR) measurement of the colorless part of **1/2** (b), the greenish part of **1/2** (c), the powder sample of **1** (d), and the powder sample of **2** (e).

crystal was analyzed by microscopic attenuated total reflectance (ATR) IR spectroscopy. The characteristic carboxylate asymmetric stretching frequencies of **1/2** (core: 1633 cm^{-1}, shell: 1621 cm^{-1}) resemble those of **1** (1629 cm^{-1}) and **2** (1621 cm^{-1}), respectively. The lower absorption energy of zinc-coordinated carboxylate relative to copper-coordinated carboxylate can be explained by the strength of carboxylate coordination; copper is coordinated more strongly than zinc.[9] Note that the multiple absorption bands around 800 cm^{-1}, which can be assigned to the out-of-plane C–H bending vibration modes and the ring bending mode of the naphthalene moieties of ndc,[10] exhibit a trend similar to the carboxylate stretching (Figure 2b–d): quadruple bands for the core and **1**; triplet bands for the shell and **2**.

Both the core crystal (**1**) and the shell crystal (**2**) have the same tetragonal space group (*P4/mmm*) and similar unit cell parameters ($a = 10.921(1)$, $c = 9.611(1)$ Å for **1**, and $a = 10.8190(3)$, $c = 9.6348(6)$ Å for **2**),[11] which differ enough, especially along the *a* axis, to distinguish the shell crystal from the core crystal and to allow investigation of the structural correlation between them. Synchrotron X-ray measurements for film structural analysis were, therefore, performed using a four-circle diffractometer at beamline BL13XU for surface and interface structures, SPring-8.

A hybridized core–shell crystal of **1/2** with a size greater than 200 μm and a shell crystal thickness greater than 20 μm was fixed on a glass surface with the *a* axis normal to the glass surface, and diffractions were recorded using an X-ray beam with a size of 15×30 μm^2. The θ–2θ scan of **1/2** from the initial position ($\chi = 90°$) provided two sharp peaks assigned to *h*00 Bragg peaks, and a scan of the rotation angle around the [100]

direction (the ϕ scan) at the 110 Bragg position gave two sharp peaks assigned to the 110 and 1−10 Bragg peaks (Figure 3a–c). These diffraction peaks indicate that the shell

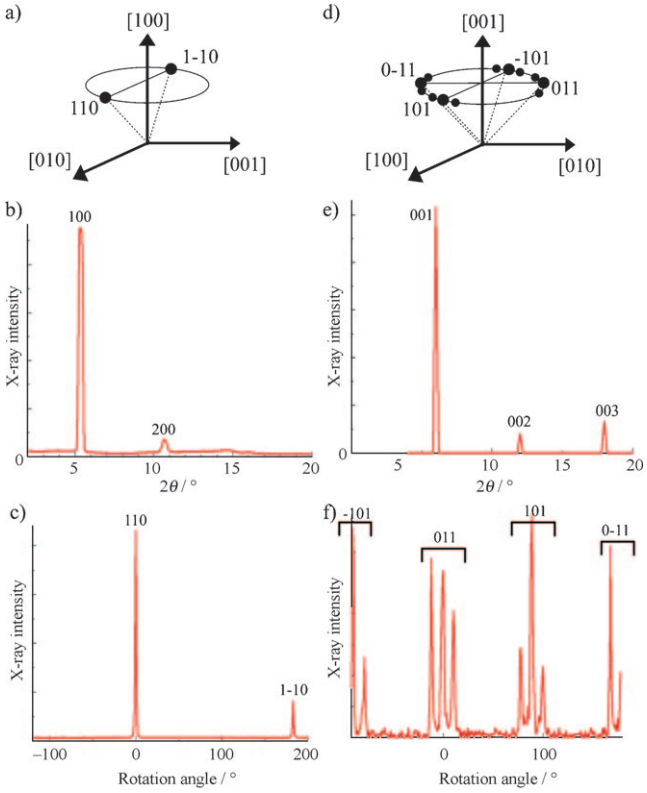

Figure 3. The reciprocal lattice space corresponding to the rotational scan a) around the [100] direction and d) around the [001] direction. The θ–2θ scan of the core–shell crystal (**1**/**2**) immobilized on the glass substrate at the initial position ($\chi = 90°$) b) along the *a* axis and e) along the *c* axis. The scan of the rotation angle c) around the [100] direction (the ϕ scan) and f) around the [001] direction.

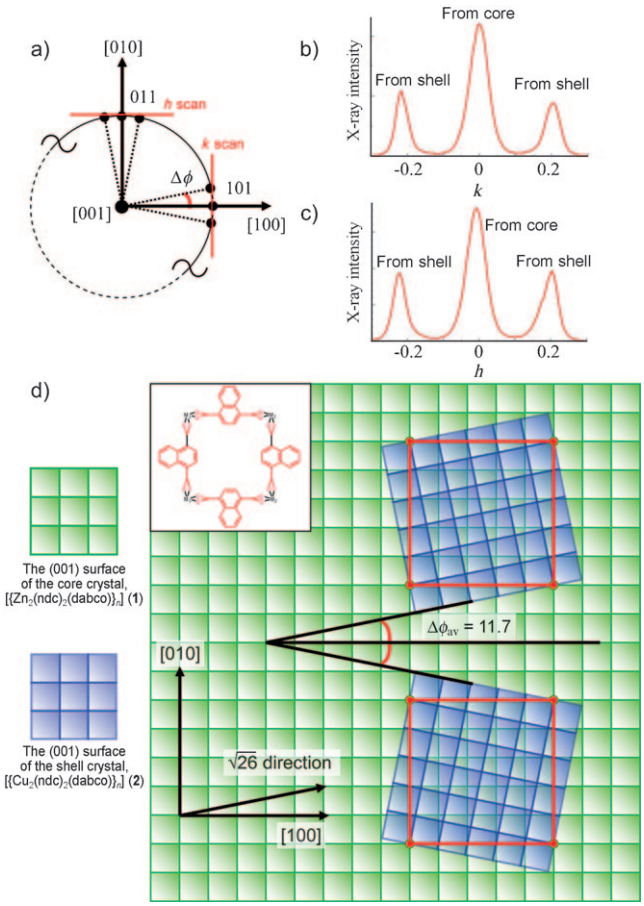

Figure 4. a) The projectional view from the [001] direction of the reciprocal lattice space. The *k* scan at the 101 position and the *h* scan at the 011 position are indicated as red lines. b) The *k* scan at the 101 position. c) The *h* scan at the 011 position. d) Schematic model of the structural relationship between the core lattice and the shell lattice on the (001) surface. The red lines indicate the commensurate lattice between the core lattice and the shell lattice; the (5×5) structure of the core crystal or the ($\sqrt{26}\times\sqrt{26}$) structure of the shell. Two Miller domains of the shell crystal are grown on the (001) surface of the core crystal while maintaining the rotational angle ($\Delta\phi_{av} = 11.6518$), which corresponds to the $\sqrt{26}$ direction of the (001) surface. The inset shows the chemical structure of the (001) surface.

crystal of **1**/**2** is a single crystal.[12] This finding indicates, surprisingly, that growth of the copper shell crystal (**2**) as a single crystal on the surface of the zinc core crystal (**1**) was supported despite the fact that the copper shell crystal had only been obtained previously as a powder.

The structural relationship between the core crystal and the shell crystal at the interface is more evident at the (001) surface, because the diffractions from the two crystals are observed simultaneously. Note that the (001) surface of the tetragonal space group can be recognized as the quadratic lattice shown in Figure 1c, because the *a* and *b* lattice constants are the same. The hybridized crystal (**1**/**2**) was mounted with the *c* axis normal to the glass surface. While the θ–2θ scan gave the 00*l* Bragg peaks, characteristic triplet peaks were observed periodically every 90° in the scan of rotation angle around [001] (the ϕ scan) at the 101 position (Figure 3d–f). Corresponding to the model in the reciprocal lattice space (Figure 4a), the *k* scan at the 101 position and the *h* scan at the 011 position also gave triplet peaks (Figure 4b–c). Each central peak of the triplet can be assigned to the 101 and 011 Bragg peaks of the core crystal (**1**), whereas the two side peaks are assigned to diffraction from the shell crystal (**2**). This situation arises because the refined 2θ angles of the side peaks ($2\theta_{side} = 8.1864$–8.1997) are significantly larger than those of the central peaks ($2\theta_{central} = 8.1136$–$8.1170$), which coincides with the fact that the lattice constant *a* of **2** is smaller than that of **1**.[13]

The difference in ϕ angle of the side peak and the central peak ($\Delta\phi$) is interpreted as rotation of the shell crystal lattice by $\Delta\phi$ with respect to the [100] direction of the core crystal lattice (Figure 4d). The result that two side peaks emerge with the central peaks, separated by similar values of $\Delta\phi$ in the *k* and *h* scans ($\Delta\phi = 11.5 \pm 0.1$ at the 101 position and $\Delta\phi = 11.7 \pm 0.6$ at the 011 position), implies that two Miller domains of the shell crystal (**2**) are grown epitaxially on the (001) surface of the core crystal (**1**) while maintaining the in-plane rotational angle $\Delta\phi$.[14] Interestingly, the average of the rotational angles ($\Delta\phi_{av} = 11.7$) reflects the angle between the

[100] direction and the $\sqrt{26}$ direction of the quadratic lattice ($\Delta\phi = 11.3$). Because the lattice constant of the shell crystal is significantly smaller than that of the core crystal, the ($\sqrt{26} \times \sqrt{26}$) structure of the shell (001) surface matches the (5×5) structure of the core crystal. Hence, in-plane rotational epitaxial growth can compensate for the difference in the lattice constants. Such rotational crystal growth evidently does not occur at the (100) surface, because the lattice constant for the [001] direction of the shell crystal is not very different from that of the core crystal, which is also evident from the lack of peak separation observed in the crystal oriented along the *a* axis. Thus, the lattice of the shell crystal matches that of the core crystal along the [100] direction by near-matched epitaxy.

These results open the way for the fabrication of hybridized PCP crystals by epitaxial growth in solution and, moreover, for the determination of the structural relationship between the shell crystal and the core crystal by surface X-ray diffraction. The surfaces of the core PCP crystal support the growth of a single-shell crystal, which was otherwise obtained only as a microcrystalline powder in the bulk. Two other layer and pillar ligands are exchangeable in this hybridization system, and functional organic ligands can be introduced. Careful choice of components should allow us to control and design the in-plane rotational angles. The next stage of progress is to correlate the interfacial structure and the function, especially the adsorption properties, which can be strongly influenced by the interfacial structure. Such rotational domain growth of a PCP crystal on the surface of the PCP core crystal apparently can work as a filter or a sieve for separation of guest molecules. Moreover, these properties originate from the formation of the interface between two PCP crystals so that the PCP framework itself can be still modified to fabricate multifunctional PCPs.

Experimental Section

Compounds **1**[6d] and **2**[6h] were prepared according to literature procedures.

Synthesis of the hybridized crystal **1/2**: A stock reaction solution of **2** was prepared from $CuSO_4 \cdot 5H_2O$ (21.0 mg, 8.41×10^{-2} mmol), ndc (as 1,4-naphthalene dicarboxylic acid; 18.2 mg, 8.42×10^{-2} mmol), and dabco (4.67 mg, 4.16×10^{-2} mmol) in toluene/methanol (5 mL, 1:1). Dozens of the core crystals **1** (sizes about $200 \times 200 \times 100\ \mu m^3$) were put into the stock reaction solution (4 mL), and the reaction mixture was heated to 393 K for 48 h. After cooling, the greenish hybridized crystals (**1/2**) were harvested.

Microscopic IR spectroscopy: The spectra were measured both by a Nicolet 6700 instrument (Thermo Fisher Scientific Inc.) with an infrared microscope (Nicolet Continuμm) and by an FTIR 6200 instrument (JASCO) with a infrared microscope (IRT-3000). An attenuated total reflection (ATR) attachment was used for the measurement. Whereas the powder samples of **1** and **2** were measured to obtain their individual spectra, the sliced single crystal sample of **1/2** was investigated for hybridization. The prism of the ATR attachment was separately put on the core and the shell of the hybrid crystal, and then each spectrum was observed.

Synchrotron X-ray measurements for film-structural analysis: Measurements were performed with a four-circle diffractometer having ϕ, χ, θ, and 2θ circles at beamline BL13XU for surface and interface structures, SPring-8. The desired crystal in DMF was selected just before measurement and fixed on the glass substrate with double-faced adhesive. Measurement was carried out under helium gas. In such conditions, guest DMF molecules most likely occupied the pores of the PCP crystal.

Details of physical measurements such as microscopic IR spectroscopy, powder X-ray diffraction measurement, and X-ray diffraction measurement for film-structural analysis are described in the Supporting Information.

Received: October 3, 2008
Published online: December 12, 2008

Keywords: coordination polymers · crystal growth · interfaces · metal–organic frameworks · microporous materials

[1] N. K. Mal, M. Fujiwara, Y. Tanaka, *Nature* **2003**, *421*, 350 – 353.
[2] a) O. M. Yaghi, M. O'Keeffe, N. W. Ockwig, H. K. Chae, M. Eddaoudi, J. Kim, *Nature* **2003**, *423*, 705 – 714; b) S. Kitagawa, R. Kitaura, S. i. Noro, *Angew. Chem.* **2004**, *116*, 2388 – 2430; *Angew. Chem. Int. Ed.* **2004**, *43*, 2334 – 2375; c) G. Férey, C. Mellot-Draznieks, C. Serre, F. Millange, *Acc. Chem. Res.* **2005**, *38*, 217 – 225; d) U. Mueller, M. Schubert, F. Teich, H. Puetter, K. Schierle-Arndt, J. Pastré, *J. Mater. Chem.* **2006**, *16*, 626 – 636; e) R. E. Morris, P. S. Wheatley, *Angew. Chem.* **2008**, *120*, 5044 – 5059; *Angew. Chem. Int. Ed.* **2008**, *47*, 4966 – 4981; f) M. Dincă, J. R. Long, *Angew. Chem.* **2008**, *120*, 6870 – 6884; *Angew. Chem. Int. Ed.* **2008**, *47*, 6766 – 6779.
[3] a) Z. Wang, S. M. Cohen, *J. Am. Chem. Soc.* **2007**, *129*, 12368 – 12369; b) Z. Q. Wang, S. M. Cohen, *Angew. Chem.* **2008**, *120*, 4777 – 4780; *Angew. Chem. Int. Ed.* **2008**, *47*, 4699 – 4702; c) K. K. Tanabe, Z. Wang, S. M. Cohen, *J. Am. Chem. Soc.* **2008**, *130*, 8508 – 8517; d) E. Dugan, Z. Wang, M. Okamura, A. Medina, S. M. Cohen, *Chem. Commun.* **2008**, 3366 – 3368; e) T. Haneda, M. Kawano, T. Kawamichi, M. Fujita, *J. Am. Chem. Soc.* **2008**, *130*, 1578 – 1579; f) Y. F. Song, L. Cronin, *Angew. Chem.* **2008**, *120*, 4713 – 4715; *Angew. Chem. Int. Ed.* **2008**, *47*, 4635 – 4637; g) J. S. Costa, P. Gamez, C. A. Black, O. Roubeau, S. J. Teat, J. Reedijk, *Eur. J. Inorg. Chem.* **2008**, 1551 – 1554; h) M. J. Ingleson, J. Perez Barrio, J. B. Guilbaud, Y. Z. Khimyak, M. J. Rosseinsky, *Chem. Commun.* **2008**, 2680 – 2682; i) J. S. Costa, P. Gamez, C. A. Black, O. Roubeau, S. J. Teat, J. Reedijk, *Eur. J. Inorg. Chem.* **2008**, 1551 – 1554.
[4] W. J. Rieter, K. M. Taylor, W. Lin, *J. Am. Chem. Soc.* **2007**, *129*, 9852 – 9853.
[5] a) P. Horcajada, C. Serre, M. Vallet-Regí, M. Sebban, F. Taulelle, G. Férey, *Angew. Chem.* **2006**, *118*, 6120 – 6124; *Angew. Chem. Int. Ed.* **2006**, *45*, 5974 – 5978; b) W. J. Rieter, K. M. Taylor, H. An, W. Lin, W. Lin, *J. Am. Chem. Soc.* **2006**, *128*, 9024 – 9025; c) B. Xiao, P. S. Wheatley, X. Zhao, A. J. Fletcher, S. Fox, A. G. Rossi, I. L. Megson, L. Regli, K. M. Thomas, R. E. Morris, *J. Am. Chem. Soc.* **2007**, *129*, 1203 – 1209; d) S. Hermes, T. Witte, T. Hikov, D. Zacher, S. Bahnmüller, G. Langstein, K. Huber, R. A. Fischer, *J. Am. Chem. Soc.* **2007**, *129*, 5324 – 5325; e) E. Biemmi, C. Scherb, T. Bein, *J. Am. Chem. Soc.* **2007**, *129*, 8054 – 8055; f) B. D. Chandler, G. Enright, D. S. Pawsey, K. Udachin, J. A. Ripmeester, D. T. Cramb, G. K. H. Shimizu, *Nat. Mater.* **2008**, *7*, 229 – 235.
[6] a) J. C. MacDonald, P. C. Dorrestein, M. M. Pilley, M. M. Foote, J. L. Lundburg, R. W. Henning, A. J. Schultz, J. L. Manson, *J. Am. Chem. Soc.* **2000**, *122*, 11692 – 11702; b) J. C. Noveron, M. S. Lah, R. E. Del Sesto, A. M. Arif, J. S. Miller, P. J. Stang, *J. Am. Chem. Soc.* **2002**, *124*, 6613 – 6625; c) S. Ferlay, W. Hosseini, *Chem. Commun.* **2004**, 788 – 789; d) E. F. Brès, S. Ferlay, P. Dechambenoit, H. Leroux, W. Hosseini, S. Reybtjens, *J. Mater. Chem.* **2007**, *17*, 1559 – 1562.
[7] a) K. Seki, W. Mori, *J. Phys. Chem. B* **2002**, *106*, 1380 – 1385; b) D. N. Dybtsev, H. Chun, K. Kim, *Angew. Chem.* **2004**, *116*,

5143 – 5146; *Angew. Chem. Int. Ed.* **2004**, *43*, 5033 – 5036; c) R. Kitaura, F. Iwahori, R. Matsuda, S. Kitagawa, Y. Kubota, M. Takata, T. C. Kobayashi, *Inorg. Chem.* **2004**, *43*, 6522 – 6524; d) H. Chun, D. N. Dybtsev, H. Kim, K. Kim, *Chem. Eur. J.* **2005**, *11*, 3521 – 3529; e) B. Q. Ma, K. L. Mulfort, J. T. Hupp, *Inorg. Chem.* **2005**, *44*, 4912 – 4914; f) B. Chen, C. Liang, J. Yang, D. S. Contreras, Y. L. Clancy, E. B. Lobkovsky, O. M. Yaghi, S. Dai, *Angew. Chem.* **2006**, *118*, 1418 – 1421; *Angew. Chem. Int. Ed.* **2006**, *45*, 1390 – 1393; g) D. Tanaka, S. Horike, S. Kitagawa, M. Ohba, M. Hasegawa, Y. Ozawa, K. Toriumi, *Chem. Commun.* **2007**, 3142 – 3144; h) T. Uemura, Y. Ono, K. Kitagawa, S. Kitagawa, *Macromolecules* **2008**, *41*, 87 – 94; i) D. Tanaka, M. Higuchi, S. Horike, R. Matsuda, Y. Kinoshita, N. Yanai, S. Kitagawa, *Chem. Asian J.* **2008**, *3*, 1343 – 1349.

[8] The yield of the hybridization was estimated as following: one hundred core crystals were used for the reaction in the same manner as described in the Experimental Section. A total of 93 light greenish (hybridized) crystals were counted out of one hundred core crystals. The yield was, thus, calculated as 93%.

[9] a) M. Bukowska-Strzyżewska, J. Skoweranda, E. Heyduk, J. Mroziński, *Inorg. Chim. Acta* **1983**, *73*, 207 – 213; b) W. Clegg, I. R. Little, B. P. Straughan, *J. Chem. Soc. Dalton Trans.* **1986**, 1283 – 1288.

[10] K. H. Michaelian, S. M. Ziegler, *Appl. Spectrosc.* **1973**, *27*, 13 – 21.

[11] These unit cell parameters for both **1** and **2** are estimated by X-ray crystal structure analyses for guest-free porous frameworks. See the Supporting Information for details of the structural analysis for **2**.

[12] Since frameworks measured herein (**1** and **1′**/**2**) most likely contained DMF molecules as guests in the pores, giving different unit cell parameters from those of the guest-free frameworks, comparison of the absolute values of each angle in Table S1 in the Supporting Information should be avoided. The difference of the lattice constant between the core crystal and the shell crystal along the *a* axis is significantly larger than that between the guest-free framework and the guest-captured framework as estimated in framework **1**, for which the crystal structures of both states have been determined.[6d] Therefore, we concluded that the effect of guest accommodation on the lattice shrinkage is negligible. See the Supporting Information for details of the comparison of the structural parameters of **1** and **2**.

[13] The 2θ angles are refined by the peaks in the $k\,o\,h$ scans, as summarized in Table S1 in the Supporting Information. The same explanation as in footnote [12] is applicable.

[14] The formation of such Miller domains on the well-defined surface is often observed in two-dimensional crystals constructed from assembled organic molecules at solid–liquid interfaces, see: a) L. Pérez-García, D. B. Amabilino, *Chem. Soc. Rev.* **2002**, *31*, 342 – 356; b) S. De Feyter, F. C. De Schryver, *Chem. Soc. Rev.* **2003**, *32*, 139 – 150.

